AIP The Journal of Chemical Physics

Thermal rate constants for the Cl+H2 and Cl+D2 reactions between 296 and 3000 K

S. S. Kumaran, K. P. Lim, and J. V. Michael

Citation: J. Chem. Phys. 101, 9487 (1994); doi: 10.1063/1.468486
View online: http://dx.doi.org/10.1063/1.468486
View Table of Contents: http://jcp.aip.org/resource/1/JCPSA6/v101/i11
Published by the American Institute of Physics.

Thermal rate constants for the Cl+H_2 and Cl+D_2 reactions between 296 and 3000 K

S. S. Kumaran, K. P. Lim, and J. V. Michael[a)]
Chemistry Division, Argonne National Laboratory, Argonne, Illinois 60439

(Received 5 July 1994; accepted 26 August 1994)

Rate constants for the Cl+H_2 and D_2 reactions have been measured at room temperature by the laser photolysis-resonance absorption (LP-RA) technique. Measurements were also performed at higher temperatures using two shock tube techniques: laser photolysis-shock tube (LP-ST) technique with Cl-atom atomic resonance absorption spectrometric (ARAS) detection, over the temperature range 699–1224 K; and higher temperature rates were obtained using both Cl-atom and H-atom ARAS techniques with the thermal decomposition of $COCl_2$ as the Cl-atom source. The combined experimental results are expressed in three parameter form as $k_{H_2}(\pm 15\%) = 4.78 \times 10^{-16} T^{1.58} \exp(-1610\ K/T)$ and $k_{D_2}(\pm 20\%) = 9.71 \times 10^{-17} T^{1.75} \exp(-2092\ K/T)$ cm^3 molecule^{-1} s^{-1} for the 296–3000 K range. The present results are compared to earlier direct studies which encompass the temperature ranges 199–1283 (H_2) and 255–500 K (D_2). These data including the present are then used to evaluate the rate behavior for each reaction over the entire experimental temperature range. In these evaluations the present data above 1300 K was given two times more weight than the earlier determinations. The evaluated rate constants are: $k_{H_2}(\pm 14\%) = 2.52 \times 10^{-11} \exp(-2214\ K/T)$ ($199 \leqslant T < 354$ K), $k_{H_2}(\pm 17\%) = 1.57 \times 10^{-16}\ T^{1.72} \exp(-1544\ K/T)$ ($354 \leqslant T \leqslant 2939$ K), and $k_{D_2}(\pm 5\%) = 2.77 \times 10^{-16}\ T^{1.62} \exp(-2162\ K/T)$ ($255 \leqslant T \leqslant 3020$ K), in molecular units. The ratio then gives the experimental kinetic isotope effect, KIE $\equiv (k_{H_2}/k_{D_2})$. Using 11 previous models for the potential energy surface (PES), conventional transition state theoretical (CTST) calculations, with Wigner or Eckart tunneling correction, are compared to experiment. At this level of theory, the Eckart method agrees better with experiment; however, none of the previous PES's reproduce the experimental results. The saddle point properties were then systematically varied resulting in an excellent model that explains all of the direct data. The theoretical results can be expressed to within $\pm 2\%$ as $k_{H_2}^{th} = 4.59 \times 10^{-16}\ T^{1.588} \exp(-1682\ K/T)$ ($200 \leqslant T \leqslant 2950$ K) and $k_{D_2}^{th} = 9.20 \times 10^{-16}\ T^{1.459} \exp(-2274\ K/T)$ cm^3 molecule^{-1} s^{-1} ($255 \leqslant T \leqslant 3050$ K). The KIE predictions are also compared to experiment. The "derived" PES is compared to a new *ab initio* calculation, and the differences are discussed. Suggestions are noted for reconciling the discrepancies in terms of better dynamics models. © *1994 American Institute of Physics.*

INTRODUCTION

As noted by Weston in 1979,[1] the reaction

$$Cl + H_2 \rightarrow HCl + H \tag{1}$$

has been of interest to chemical kineticists since the pioneering work of Nernst.[2] This reaction and its isotopic variations including

$$Cl + D_2 \rightarrow DCl + D \tag{2}$$

have served as test cases for bimolecular reaction rate theory,[1] particularly transition state theory[3] and the theory of isotope effects that is derived from it.[4] The accurate derivation of a potential energy surface for the interaction has been a major undertaking, and the success of theory has been hampered by an inexact knowledge of this surface. Many surfaces have been derived including those using London–Eyring–Polanyi and/or Sato (LEP and/or LEPS), and various versions of diatomics in molecules (DIM) methods.[5] Tucker *et al.*[5] have then calculated thermal rate constants and isotope effects for 11 different surfaces using both conventional and variational transition state theory along with separate procedures for including tunneling factors.

The experimental work that has prompted the substantial theoretical interest is likewise extensive. The NIST database[6] lists 16 prior studies of Reaction (1), 6 of which are direct determinations.[7–12] The temperature range encompassed by these studies is 199–500 K; however, this range has been extended to 1283 K in a recent study by Adusei and Fontijn.[13] The data on Reaction (2) is much less extensive. Miller and Gordon have reported data between 202–499 K[14] and have extensively discussed the kinetic isotope effect for Reactions (1) and (2) in terms of their own data and theoretical models.

Even though Reaction (1) has some practical interest in atmospheric chemistry and has been used as a "known" reaction in competitive studies, our motivation for the present work is mostly theoretical. Experimental comparisons of thermal rate data with theory have been an ongoing theme in several studies from this laboratory including both the protonated and deuterated modifications of the H+H_2, O+H_2,

[a)]Author to whom correspondence should be addressed.

TABLE I. Rate data for $Cl+H_2 \rightarrow HCl+H$ and $Cl+D_2 \rightarrow DCl+D$ at 296 K.

P_1/(Torr)		k_{first}/(s^{-1})		k/(10^{-15} cm^3 s^{-1})
	$X_{COCl_2} = 2.704 \times 10^{-4}$		$X_{H_2} = 1.720 \times 10^{-2}$	
199.3		2199		19.6
241.1		2571		19.0
	$X_{COCl_2} = 2.832 \times 10^{-4}$		$X_{H_2} = 4.106 \times 10^{-2}$	
65.3		1282		14.6
65.3		1550		17.7
112.8		2634		17.4
155.1		3109		15.0
155.1		2923		14.1
				Ave.=16.8±2.2
	$X_{COCl_2} = 2.727 \times 10^{-4}$		$X_{D_2} = 9.809 \times 10^{-2}$	
96.9		681		2.20
154.8		664		1.34
207.9		1247		1.87
237.7		1331		1.75
				Ave.=1.79±0.35

$O+C_2H_2$, $H+H_2O$, and $H+O_2$ reactions.[15–18]

Except for determinations at 296 K, the present results for Reactions (1) and (2) were obtained using shock tube methods. Two types of shock tube experiments were employed, one using the thermal dissociation of $COCl_2$[19] as a thermal Cl-atom source at high temperatures, and the other using the laser photolysis-shock tube (LP-ST) technique.[16,17] The photochemical source in these latter experiments was also $COCl_2$. In both types of studies, Cl atoms were monitored by Cl-atom atomic resonance absorption spectroscopy (ARAS).[19,20] Including the room temperature results, data have been obtained for both reactions over the large temperature range 296 to 3000 K, and these are combined with earlier lower temperature results to give evaluations over the entire temperature range of the collective experiments, ~200–3000 K. Since this study substantially extends the upper temperature range for the title reactions, it places additional constraints on a successful theoretical description.

EXPERIMENT

The experimental method, apparatus, and techniques that are used in the present study have been completely described elsewhere.[16,17] Therefore a few pertinent additional comments will suffice.

Apparatus

The shock tube equipment used here is comprised of a driver chamber and a 7 m 304 stainless-steel tube (i.d. 9.74 cm) section, the inside surface of which has been polished to be quite passive. These two sections are separated by a thin aluminum diaphragm (4 mil, unscored 1100-H18). This is mounted between vacuum flanges that are attached to the ends of the driver and driven sections. The tube was routinely pumped by an Edwards Vacuum Products Model CR100 *P* fore-pump diffusion-pump combination to $<10^{-8}$ Torr before loading the test gas. Reaction mixtures were prepared manometrically with an MKS Baratron capacitance manometer. Initial reactant loading pressures were also measured with the manometer. Shock waves were produced by rapidly cutting a 2.25 in. square in the diaphragm. Except for the room temperature experiments of Table I, all other experiments were carried out in the reflected shock wave regime. The average incident shock velocity for each experiment was obtained with fast piezoelectric transducers (PCB Piezotronics, Inc., Model 1132 A) at eight different stations that are equally spaced well downstream from the diaphragm. The thermodynamic properties shown in Tables II and III were calculated from these velocities with appropriate Mirels' boundary layer corrections as described earlier.[16,21,22] As in previous studies,[16,19,22,23] the photometer system was radially located 6 cm from the end plate, and the optical path length was 9.94 cm. As shown in the tables, the experiments were performed with varying mixture compositions. The Cl-atom ARAS technique was used to measure rate constants for Reactions (1) and (2). Additionally, the H-atom ARAS method was used to measure total [H] yields from Reaction (1). In both types of experiments, transmittances from the resonance lamps were measured with a solar blind EMR G14 photomultiplier tube, and the signals were recorded and stored for kinetics analyses with a Nicolet 4094C digital oscilloscope.

H-atom ARAS detection

The application of the ARAS technique for measuring [H] is well established,[24–27] and the photometer system used here has been completely characterized[27] and used in earlier shock tube investigations.[28–35] Ly_α radiation was generated in the resonance lamp with a microwave discharge operating at 40 W in prepurified grade He flowing at a total pressure of 2 Torr. There are sufficient H atom containing impurities in this grade of He to give an easily measurable Ly_α signal. Under these conditions line reversal is negligible.[27] Before each experiment the fraction of non-Ly_α light was measured through an O_2 (1 atm of dry air) gas filter using an atomic filter section that was essentially a fast flow system in which a large H-atom concentration could be generated with a second microwave discharge located upstream from the optical path.

In a recent study from this laboratory on the methyl-

TABLE II. High-temperature rate data for $Cl+H_2 \rightarrow HCl+H$ and $Cl+D_2 \rightarrow DCl+D$.

P_1/(Torr)	M_s[a]	$\rho_5/(10^{18}\ cm^{-3})$[b]	T_5/(K)[b]	$k/(10^{-11}\ cm^3\ s^{-1})$[c]	K_{eq}
	$X_{COCl_2} = 6.624 \times 10^{-6}$		$X_{H_2} = 7.511 \times 10^{-5}$		
15.98	2.839	3.399	1957	3.05	1.68
15.89	2.724	3.285	1809	2.50	1.97
15.91	2.978	3.503	2136	4.50	1.73
15.92	3.033	3.548	2209	5.30	1.72
15.95	3.044	3.563	2222	5.00	1.73
15.91	3.123	3.613	2330	6.10	1.81
15.90	3.402	3.795	2728	7.00	
15.95	3.159	3.648	2379	7.00	1.37
15.88	3.122	3.606	2328	5.80	1.66
10.93	2.684	2.237	1784	2.30	1.24
10.92	2.962	2.431	2135	3.60	1.38
10.97	2.996	2.454	2189	5.50	1.21
10.91	3.127	2.517	2373	5.80	1.34
10.88	3.396	2.647	2772	7.30	
10.95	3.198	2.565	2474	6.35	1.40
10.94	3.052	2.481	2267	5.50	1.59
10.91	2.914	2.391	2079	4.30	1.52
10.89	2.861	2.352	2009	4.00	1.49
10.95	2.764	2.299	1884	3.00	1.57
	$X_{COCl_2} = 1.995 \times 10^{-5}$		$X_{H_2} = 7.535 \times 10^{-5}$		
15.90	2.820	3.378	1927	3.20	1.25
15.90	3.169	3.657	2386	6.20	1.37
15.96	2.992	3.537	2147	5.20	1.20
15.95	3.007	3.534	2173	4.70	1.19
10.98	3.115	2.535	2347	4.50	1.01
10.94	2.992	2.454	2176	3.70	0.98
10.96	2.816	2.345	1944	2.70	0.87
10.92	2.779	2.311	1896	2.30	1.00
	$X_{COCl_2} = 6.602 \times 10^{-6}$		$X_{H_2} = 7.680 \times 10^{-5}$		
15.92	2.714	3.249	1816	2.70	1.89
15.97	2.822	3.360	1949	3.05	2.09
15.88	2.810	3.300	1934	3.30	2.11
15.86	2.851	3.362	1985	3.45	1.73
15.88	3.528	3.836	2939	9.00	
15.96	2.839	3.373	1971	3.55	1.90
15.89	2.833	3.352	1962	3.55	2.08
15.94	2.845	3.373	1978	3.30	1.93
15.90	2.692	3.224	1790	2.30	1.58
15.98	2.835	3.373	1965	2.90	1.87
15.92	2.675	3.211	1769	2.00	1.94
15.92	2.755	3.288	1866	2.50	1.81
15.83	2.742	3.257	1850	2.53	1.83
15.87	2.732	3.256	1838	2.53	1.85
15.88	3.024	3.508	2211	5.10	2.00
15.92	2.685	3.231	1775	2.50	1.20
	$X_{COCl_2} = 1.290 \times 10^{-5}$		$X_{H_2} = 8.400 \times 10^{-5}$		
15.88	2.805	3.337	1921	2.95	1.30
15.86	2.831	3.356	1954	3.10	1.40
15.90	2.959	3.473	2118	3.90	1.50
15.91	2.994	3.504	2164	4.50	1.37
15.90	2.986	3.495	2153	4.15	1.37
15.88	3.312	3.722	2605	6.10	1.39
15.89	3.449	3.808	2808	8.10	
10.89	3.073	2.482	2296	5.10	1.43
10.92	2.999	2.446	2194	4.50	1.52
10.90	2.963	2.419	2144	4.35	1.54
10.91	2.847	2.347	1990	3.45	1.70
10.94	2.796	2.319	1925	3.15	1.65
10.91	2.737	2.272	1850	2.30	1.29
5.93	3.064	1.349	2283	5.20	1.65
5.91	2.889	1.282	2052	3.70	1.29
5.91	3.070	1.341	2299	4.85	1.65
5.88	3.163	1.363	2432	5.80	2.00
5.93	3.188	1.381	2468	5.97	1.49
5.89	3.088	1.342	2324	5.13	1.71

TABLE II. (*Continued.*)

P_1/(Torr)	M_s[a]	$\rho_5/(10^{18}\ cm^{-3})$[b]	T_5/(K)[b]	$k/(10^{-11}\ cm^3\ s^{-1})$[c]	K_{eq}
	$X_{COCl_2} = 6.648 \times 10^{-6}$		$X_{D_2} = 7.621 \times 10^{-5}$		
10.92	3.033	2.465	2239	3.30	1.23
10.81	3.139	2.500	2389	3.80	1.52
10.91	3.476	2.691	2897	5.00	1.72
10.91	3.243	2.579	2540	3.85	1.53
11.00	3.014	2.481	2207	2.80	1.57
10.85	2.920	2.387	2086	2.35	1.28
10.89	2.838	2.336	1978	2.00	1.31
10.94	2.824	2.346	1954	2.00	1.14
15.96	2.930	3.462	2080	3.00	1.25
15.92	2.937	3.459	2089	2.70	1.50
15.96	2.808	3.356	1925	2.00	1.13
15.94	3.180	3.648	2416	3.80	1.30
15.88	3.244	3.678	2508	3.98	1.50
15.94	3.171	3.642	2404	4.80	0.98
15.99	3.248	3.706	2513	4.30	1.51
15.96	2.750	3.302	1853	1.60	1.66
15.98	2.608	3.165	1684	1.20	1.40
	$X_{COCl_2} = 1.539 \times 10^{-5}$		$X_{D_2} = 9.928 \times 10^{-5}$		
10.91	3.064	2.482	2283	2.30	0.65
10.98	3.405	2.676	2786	4.00	1.10
10.88	2.711	2.247	1817	1.31	0.51
10.88	2.857	2.347	2003	1.64	0.67
10.92	3.012	2.445	2219	2.50	0.80
5.96	3.547	1.482	3020	5.00	1.35
5.97	3.005	1.334	2209	2.86	0.71
5.98	3.206	1.399	2495	3.47	0.92
5.97	3.089	1.357	2334	3.35	0.98
5.94	2.982	1.316	2184	2.97	1.04
5.93	2.855	1.270	2015	2.22	0.83

[a]The error in measuring the Mach number M_s is typically 0.5%-1.0% at the one standard deviation level.
[b]Quantities with the subscript 5 refer to the thermodynamic state of the gas in the reflected shock region.
[c]The rate constants are derived as described in the text.

radical dissociative-recombination reaction,[36] H-atom calibration experiments were reported. Line absorption calculations for a Doppler broadened and slightly reversed source at a lamp temperature of 480 K[27] were carried out using the known oscillator strength for the $^2P_{3/2,1/2} \leftarrow {}^2S_{1/2}$ H-atom transition. It was shown that the H-atom yield from C_2H_5I pyrolysis experiments was within 20% of that inferred from the calculations. Also, calibration experiments using Reaction (1) were reported.[36] In these experiments, various loading pressures of a mixture with mole fractions, $X_{COCl_2} = 1.718 \times 10^{-7}$ and $X_{H_2} = 1.986 \times 10^{-4}$ in Kr, were shock heated between 1784–2381 K, and $(ABS)_H = -\ln(I/I_0)$ was measured as a function of time. These values were converted to an $[H]_t$ profile through a line absorption calculation for the experimental temperature. It was necessary to fit these profiles with the chemical mechanism[37–40] shown in Table IV. We concentrated on the long time H-atom yields from these experiments. For the high-temperature conditions here, the yield was independent of the $COCl_2$ dissociation rate (i.e., dissociation was effectively instantaneous on the experimental time scale) and thus depended only on $[COCl_2]_0$. The only two reactions that are important under these low $[COCl_2]_0$ conditions are Reaction (1) and the thermal dissociation of H_2, the third reaction in Table IV. In earlier work from this laboratory,[19] we found that $COCl_2$ gives 1.808 Cl atoms for every molecule decomposed with the molecular channel, $COCl_2 \rightarrow CO + Cl_2$, contributing the remaining 9.6% to the depletion. Therefore, $[Cl]_0$ in the chemical simulations using Table IV was taken as 1.808 $[COCl_2]_0$. The simulated H-atom profiles were then compared to those from measured absorbances converted to $[H]_t$ through the line absorption calculations,[27] and the results are presented in Fig. 1. The line shown in the figure has the slope (0.99 ± 0.03) indicating complete consistency between [H] from line absorption calculations and that derived from known $[COCl_2]_0$ (and therefore $[Cl]_0$) through Reaction (1). Finally, since the determination of the Cl-atom yield as a function of $[COCl_2]_0$ in our earlier work[19] required a knowledge of the Cl-atom curve of growth,[41,42] the present results for H-atom yields are entirely consistent, within experimental error, to those for Cl-atom yields, and, therefore, the relative relationship between the H-atom and Cl-atom curves of growth can now be considered to be known through the described calibration procedure.

Cl-atom ARAS detection

The Cl-atom resonance lamp has been detailed in recent studies.[19,20,23,41,42] The lamp operates at 50 W microwave power in a 2.0 Torr flowing mixture of $X_{Cl_2} = 10^{-3}$ in He.

TABLE III. Rate data for Cl+H_2 and Cl+D_2 by the LP-ST technique.

P_1/(Torr)	M_s[a]	$\rho_5/(10^{18}\ cm^{-3})$[b]	T_5/(K)[b]	$k_{first}/(s^{-1})$	$k/(10^{-12}\ cm^3\ s^{-1})$[c]
	$X_{COCl_2} = 1.292\times10^{-4}$		$X_{H_2} = 3.551\times10^{-4}$		
15.99	2.053	2.468	1102	4800	5.48
15.86	2.036	2.468	1086	5398	6.27
15.90	1.913	2.238	975	3666	4.61
15.96	1.872	2.179	939	3272	4.23
15.96	1.641	1.777	751	1185	1.88
15.84	1.710	1.887	805	2121	3.16
15.90	1.574	1.647	699	1276	2.18
15.98	1.886	2.204	951	3196	4.08
15.80	1.808	2.051	885	2411	3.31
15.90	1.880	2.184	946	3268	4.21
10.97	2.027	1.651	1071	3398	5.79
10.90	2.171	1.790	1211	4883	7.68
10.96	1.954	1.679	1097	4553	7.64
10.92	2.006	1.621	1051	2926	5.08
10.89	1.871	1.465	930	2199	4.23
10.98	1.836	1.436	900	2707	5.31
	$X_{COCl_2} = 6.085\times10^{-5}$		$X_{H_2} = 6.690\times10^{-4}$		
15.91	1.755	1.973	841	3145	2.38
15.86	1.682	1.839	782	2473	2.01
15.85	1.642	1.766	751	2404	2.04
15.79	2.035	2.410	1085	12704	7.88
15.91	1.985	2.353	1039	8693	5.52
15.90	1.904	2.223	967	7904	5.31
15.95	1.872	2.177	939	6538	4.49
15.96	1.790	2.041	870	3757	2.75
15.84	1.787	2.021	868	5144	3.80
	$X_{COCl_2} = 1.324\times10^{-4}$		$X_{H_2} = 3.121\times10^{-4}$		
10.94	2.143	1.763	1187	5374	9.77
10.93	2.003	1.614	1053	3084	6.12
10.84	2.180	1.796	1217	4332	7.73
10.97	2.088	1.722	1126	4105	7.64
10.90	1.992	1.603	1039	3574	7.14
10.91	1.988	1.600	1035	3437	6.88
10.93	1.866	1.464	925	2268	4.96
15.81	2.004	2.359	1060	3094	4.20
15.90	1.850	2.135	921	2223	3.34
15.82	1.794	2.029	873	1679	2.65
	$X_{COCl_2} = 1.245\times10^{-4}$		$X_{D_2} = 3.130\times10^{-5}$		
10.90	2.163	1.777	1207	2030	3.65
10.94	2.037	1.658	1081	1303	2.51
10.89	1.916	1.517	970	930	1.96
10.88	1.762	1.329	839	626	1.51
10.84	1.981	1.577	1032	1196	2.42
10.93	2.031	1.644	1079	1487	2.89
10.83	2.121	1.723	1165	1857	3.44
10.97	2.184	1.815	1224	1820	3.20
15.82	2.079	2.481	1127	2285	2.94
15.85	1.878	2.166	948	1279	1.89
15.91	1.784	2.024	865	485	0.77
15.81	1.811	2.057	887	1128	1.75
15.95	1.880	2.191	946	696	1.01
15.97	2.029	2.429	1079	2055	2.70
15.85	2.018	2.394	1069	1495	2.00
	$X_{COCl_2} = 6.326\times10^{-5}$		$X_{D_2} = 6.346\times10^{-4}$		
15.84	1.808	2.049	888	2740	2.11
15.86	1.726	1.911	821	1025	0.85
15.92	1.742	1.946	833	1661	1.35
15.85	1.929	2.248	992	2748	1.93
15.91	1.950	2.291	1012	2594	1.78
15.85	1.819	2.075	894	2355	1.79
30.88	1.866	4.088	918	3781	1.46
30.79	1.789	3.826	853	2859	1.18
30.57	1.671	3.406	759	1628	0.75
30.77	1.710	3.561	790	1692	0.75

[a]The error in measuring the Mach number M_S is typically 0.5%–1.0% at the one standard deviation level.
[b]Quantities with the subscript 5 refer to the thermodynamic state of the gas in the reflected shock region.
[c]The rate constants are derived as described in the text.

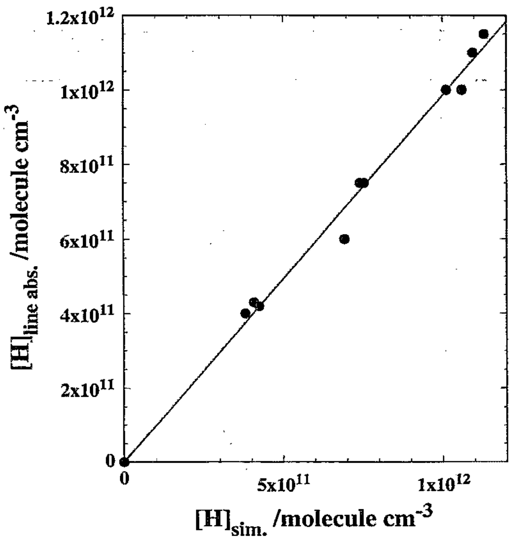

FIG. 1. Calibration plot for the H-atom ARAS method. [H], obtained from converting measured absorbances through line absorption calculations, is plotted against [H] determined from the Table IV reaction mechanism. The nearly unit slope indicates consistency with the known oscillator strength for the $^2P_{3/2,1/2} \leftarrow {}^2S_{1/2}$ transition in H and also gives the relative relationship between the H-atom and Cl-atom curves of growth.

As discussed by Clyne and Nip[43] and Whytock *et al.*,[44] this resonance lamp gives a multiplet structure that is somewhat reversed. The resonance radiation was observed through a BaF_2 filter without wavelength resolution over the range 133.6–139.6 nm. From pyrolytic studies of CCl_4,[41] this lamp configuration gives (14±2)% nonresonance radiation, and a knowledge of this factor then allows $(ABS)_{Cl}$ to be determined. Thermal dissociation experiments with a variety of Cl-atom source molecules have been performed in this laboratory,[19,20,23,41,42] and the curve of growth has been determined. Based on near linear behavior for $0 \leqslant (ABS)_{Cl} \leqslant 0.1$, the effective Cl-atom absorption cross section is $(2.37 \pm 0.08) \times 10^{-15}$ cm^2. However, since the curve of growth becomes highly nonlinear at $(ABS)_{Cl} \geqslant 0.1$, a modified Beer's law expression has been derived,[45]

$$(ABS)_{Cl} = 4.41 \times 10^{-9} [Cl]^{0.582}, \tag{3}$$

where [Cl] is expressed in atoms cm^{-3}.

In the present study, $COCl_2$ was the Cl-atom source in the shock tube experiments. Depending on the temperature range, two types of experiments were performed. For temperatures greater than 1769 K, the thermal dissociation of $COCl_2$ supplied 1.808 atoms per dissociated molecule. In this experiment, the measured absorbances were generally above 0.1 for most of the temporal change, and therefore, Eq. (3) was used to derive the temporal profiles. We also performed LP-ST experiments using 193 nm ArF excimer laser light to photodissociate $COCl_2$. These experiments were carried out below 1224 K in order to inhibit Cl-atom formation from thermal dissociation. In this experiment, initial absorbances were limited to <0.08. Hence, first-order decay plots could be directly determined from absorbances since $(ABS)_{Cl}$ is linearly proportional to [Cl] in this range.

Gases

The He driver gas (99.995%) was obtained from Air Products and Chemicals, Inc. Scientific grade Ar (99.9999%) and Kr (99.997%), both from MG Industries, were used as the diluent gases in the reaction mixtures. Scientific grade H_2 (99.9999%) was also obtained from MG Industries whereas D_2 was scientific grade (99.99% with only 16.5 ppm nonhydrogenous impurities) from Air Products and Chemicals, Inc. Both were used without further purification. Electronic grade Cl_2 (99.999%) from MG Industries, diluted in ultrahigh purity He (99.999%) from Airco Industrial Gases, was used in the Cl-atom resonance lamp. $COCl_2$ (99.0%) was obtained from AGA Specialty Gases and was purified by bulb-to-bulb distillation. The middle third was retained for mixture preparation.

RESULTS

Room temperature experiments

Rate constant determinations for Reactions (1) and (2) were carried out in Ar diluent at 296 K using the shock tube as a static reactor. The single shot laser photolysis-resonance absorption (LP-RA) method was used for the conditions shown in Table I. Initial $(ABS)_{Cl} \leqslant 0.09$ ensured that Beer's law would hold. Since $(ABS)_t = \sigma_{Cl} l [Cl]_t$ and $[Cl]_0 \ll [H_2]$ or $[D_2]$, the decay of atoms will be pseudo-first-order; i.e.,

$$\ln(ABS)_t = -k_1[H_2]t + c \quad \text{or} \quad -k_2[D_2]t + c'. \tag{4}$$

Plots of the left-hand side of Eq. (4) against time give the decay constants k_{first} in the table, and these yield the bimolecular rate constants k_1 or k_2 when divided by $[H_2]$ or $[D_2]$. Diffusional loss, which is normally subtracted from the observed decay constants, is not important in the present experiments since the pressures are relatively high and diffusion is slow in comparison to the observed decay constants. The average values of the 296 K rate constants are included in the Figs. 2 and 3 Arrhenius plots.

Thermal dissociation experiments

These shock tube experiments were performed with Kr diluent using the thermal dissociation of $COCl_2$ as the source of Cl atoms. The upper panel of Fig. 4 shows an example of a raw data signal. It was necessary to use Eq. (3) to convert the raw data to $[Cl]_t$ since the $(ABS)_t$ values ranged well into the nonlinear curve-of-growth region [i.e., up to (ABS) $\cong$0.4]. The resulting Cl-atom profile is shown as the bottom panel, and it is obvious from the figure that Reaction (1) or (2) and their reverse reactions are equilibrating at long times. This is a direct observation of the reversibility of the processes, and the behavior was noted for all the experiments shown in Table II.

The question arises as to whether the observed levels of $[Cl]_\infty$ are consistent with known equilibrium constants for the system. From the data, approximate values for the equilibrium constants can be calculated from

$$K_{eq} = \frac{([Cl]_0 - [Cl]_\infty)^2}{\{[H_2]_0 - ([Cl]_0 - [Cl]_\infty)\}[Cl]_\infty}, \tag{5}$$

TABLE IV. Reaction mechanism used for deriving the high-temperature rate constants for $Cl+H_2$.[a]

1.	$Cl+H_2 \rightarrow HCl+H$	k_1=to be fitted
2.	$H+HCl \rightarrow H_2+Cl$	$k_2=k_1/K^1_{eq}$=to be fitted
3.	$H_2(+M) \rightarrow 2H(+M)$	$k_3=\rho \times 8.86 \times 10^{-10} \exp(-48\,321\ K/T)$[b]
4.	$HCl(+M) \rightarrow H+Cl(+M)$	$k_4=\rho \times 6.97 \times 10^{-11} \exp(-40\,765\ K/T)$[c]
5.	$H+Cl_2 \rightarrow HCl+Cl$	$k_5=1.43 \times 10^{-10} \exp(-590\ K/T)$[d]
6.	$Cl+HCl \rightarrow H+Cl_2$	$k_6=k_5/[2.14 \exp(23\,532\ K/T)]$[e]

[a]All rate constants are in molecular units.
[b]Reference 37.
[c]Reference 38.
[d]Reference 39.
[e]Equilibrium constant calculated from data in Ref. 40.

where $[Cl]_0=1.808\ [COCl_2]_0$. $[Cl]_\infty$ was determined either with the linear expression for $(ABS)_{Cl} \leq 0.1$ or from Eq. (3) for $(ABS)_{Cl}>0.1$. However, since other processes can potentially affect $[Cl]_\infty$ (e.g., the thermal decomposition of HCl), it was necessary to simulate the kinetics with the mechanism shown in Table IV. The approximate values for K_{eq} from Eq. (5) served as the starting values for these simulations, and both this quantity and the rate constant for Reaction (1) were parametrically varied to obtain the best fit to the profile. The resulting values for K_{eq} are reported in Table II and are plotted in Fig. 5 for both Reactions (1) and (2). Between 700–2700 K, the *JANAF Thermodynamic Data Tables*[40] give the van't Hoff expressions

$$K_{1\ eq}=1.689 \exp(-450.9\ K/T) \tag{6}$$

and

$$K_{2\ eq}=1.833 \exp(-811.9\ K/T) \tag{7}$$

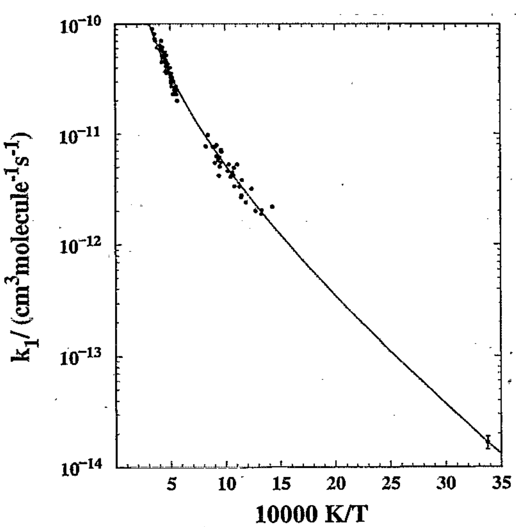

FIG. 2. Arrhenius plot of measured rate constants for the $Cl+H_2 \rightarrow HCl+H$ reaction. The data are as follows: $1769 \leq T \leq 2939$ K are the thermal dissociation experiments, $699 \leq T \leq 1217$ K are the LP-ST experiments. The data at 296 K as given in Table I are also shown. The solid line represents the three parameter least-squares fit, Eq. (8), over the experimental temperature range $296 \leq T \leq 2939$ K.

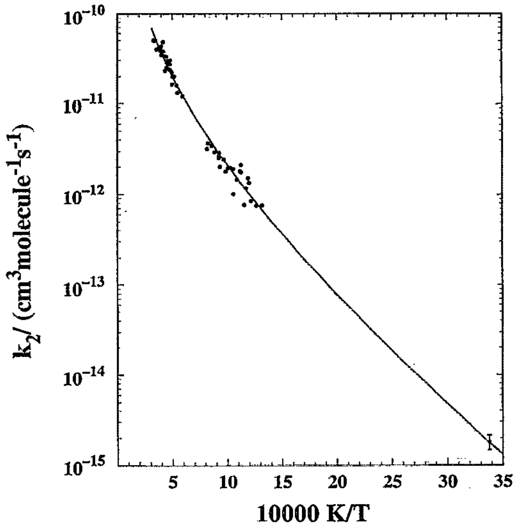

FIG. 3. A plot analogous to Fig. 2 for the isotopic variation, $Cl+D_2 \rightarrow DCl+D$. Here the data are $1684 \leq T \leq 3020$ K, thermal dissociation experiments; $759 \leq T \leq 1224$ K, the LP-ST experiments; and the rate constant at 296 as given in Table I are also shown. The solid line is again a least-squares fit to the data, Eq. (9), over the range $296 \leq T \leq 3020$ K.

to within 1%. The lines shown in the figure are calculated from Eqs. (6) and (7). For both reactions, there are system-

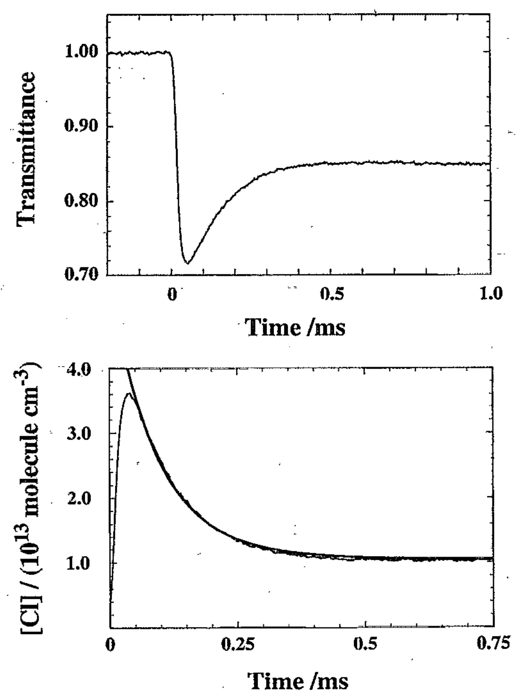

FIG. 4. A typical record from a thermal dissociation experiment. The experimental conditions and composition are $T_5=2194$ K, $P_5=556$ Torr, $\rho_5=2.446 \times 10^{18}\ cm^{-3}$, X_{COCl_2} = 12.90 ppm, and X_{H_2} = 84.00 ppm. The ARAS signal (top panel) shows the Cl-atom depletion following its rapid formation from the decomposition of $COCl_2$. The absolute [Cl] profile (bottom panel) is obtained by converting the raw data (top panel) as described in the text. The smooth solid line is the model calculation for [Cl] using the Table IV reaction mechanism.

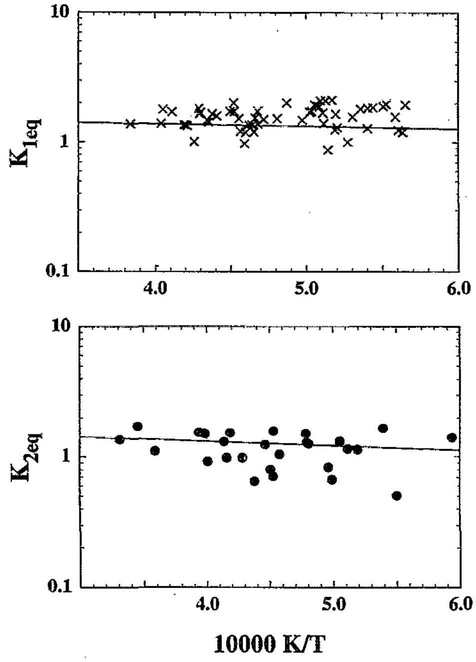

FIG. 5. van't Hoff plots of equilibrium constants for Cl+H_2⇌HCl+H (top) and Cl+D_2⇌DCl+D (bottom), derived from the mechanism of Table IV. The solid lines are the respective van't Hoff expressions derived from the *JANAF* tables.

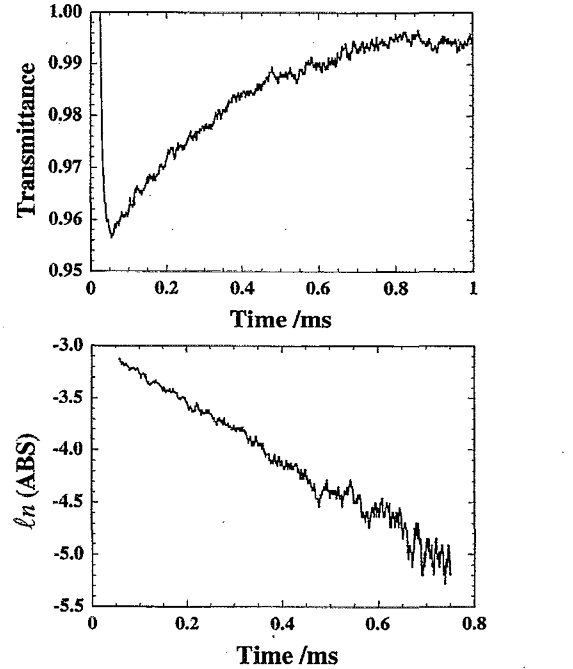

FIG. 6. A typical LP-ST experimental record. Conditions and composition are T_5=992 K, P_5=231 Torr, $\rho_5=2.248\times10^{18}$ cm^{-3}, X_{COCl_2} = 63.26 ppm, and X_{D_2} = 634.6 ppm. The top panel shows the Cl-atom transmittance following its formation from photolysis of $COCl_2$. The bottom panel shows the corresponding $(ABS)_{Cl}$ profile. For $(ABS)_{Cl}<0.08$, the $(ABS)_{Cl}$ vs [Cl] relationship is linear, and the linear semilog absorption profile then directly yields the pseudo-first-order decay constant, $k_{first}=2748$ s^{-1}.

atic differences between the mixtures, with those higher in $COCl_2$ giving slightly lower values. These differences are not serious since an error of ±25% in each determination of K_{eq} can easily be justified through an error propagation analysis if the following are considered: (i) Probable inaccuracies in the H_2 and HCl thermal decompositions [Reactions (3) and (4) in Table IV]; (ii) the long extrapolation in T^{-1} for Reaction (5) in the table; and (iii) the one standard deviation uncertainty of ±8% in the Cl-atom curve of growth.[42,45] Therefore, the significant conclusions from these determinations are that they prove reversibility and closely corroborate the *JANAF* implied values[40] for the Reactions (1) and (2) equilibrium constants.

As mentioned above, k_1 or k_2 was iteratively varied to best fit the experimental [Cl] profile, with the mechanism of Table IV. A typical fit is shown in Fig. 4 as the solid line. We concentrated on the $[Cl]_t$ decay region between ~1 to ~7×10^{13} cm^{-3} because of the above noted inaccuracies in the secondary chemistry and curve of growth. Under these conditions, the only important reactions are Reactions (1) and (2) and their backreactions, and changes of ±10% in k_1 or k_2 typically gave worse fits to the profile data. For many runs, we expanded the mechanism by explicitly including both channels for the thermal dissociation of $COCl_2$ (i.e., CO+Cl_2 and COCl+Cl with the subsequent fast dissociation, COCl→CO+Cl).[19] For the present temperature range, the relative profiles with and without this expansion were exactly the same, with the decay of $[Cl]_t$ to $[Cl]_\infty$ simply being delayed. The reason for this behavior is that the source, $COCl_2$, had totally reacted well before $[Cl]_t$ decayed. We therefore used $[Cl]_0=1.808$ $[COCl_2]_0$ and $[Cl_2]_0=0.096$ $[COCl_2]_0$ for each experiment with its given value of temperature, density, and $[H_2]_0$ or $[D_2]_0$, as starting conditions in the simulations used for deriving the rate constants. The final results are given in Table II and are plotted in Figs. 2 and 3.

LP-ST experiments

These shock tube experiments with Ar diluent were straightforward and followed procedures described previously.[16,17] The photolyte was $COCl_2$, and its relatively low absorption cross section at 193 nm[46] required that relatively high concentrations be used even with a laser energy of ~250 mJ. At this high concentration, the onset of thermal decomposition giving Cl atoms then determined the higher temperature limit (1224 K) for these experiments. The top panel of Fig. 6 shows a typical raw data record. In all such experiments, initial $(ABS)_{Cl}$ was <0.08. Therefore the photometer behavior was in the linear portion of the curve of growth. Hence, the data were analyzed according to Eq. (4). The Fig. 6 top panel result then yields the semilog decay plot in the lower panel. The observed first-order decay constants from the negative slopes of such plots for 35 H_2 and 25 D_2 experiments are given in Table III along with the derived values of k_1 and k_2. These LP-ST results are also included in Figs. 2 and 3.

Three parameter expressions of the form $k=AT^n\exp(-B/T)$ have been determined by least-squares methods for the composite sets of data shown in Figs. 2 and 3. The results are

$$k_1=4.78\times10^{-16}T^{1.58}\times\exp(-1610\ \text{K}/T)\ \text{cm}^3\,\text{molecule}^{-1}\,\text{s}^{-1} \quad (8)$$

and

$$k_2=9.71\times10^{-17}T^{1.75}\times\exp(-2092\ \text{K}/T)\ \text{cm}^3\,\text{molecule}^{-1}\,\text{s}^{-1}. \quad (9)$$

These two expressions are plotted in Figs. 2 and 3, respectively. The data in Fig. 2 deviate from Eq. (8) by ±15% whereas those in Fig. 3 deviate from Eq. (9) by ±20%, both at the one standard deviation level.

DISCUSSION

Comparison to earlier work

The present results can be compared to previous direct studies. Our room temperature result for Reaction (1), $k_1=(1.68\pm0.22)\times10^{-14}$ $\text{cm}^3\,\text{molecule}^{-1}\,\text{s}^{-1}$, agrees well with all earlier studies; i.e., (1.34±0.07),[7] (1.40±0.10),[8] (1.80±0.20),[9] (1.50±0.30),[10] (1.66±0.11),[11] (1.46±0.22),[12] and (1.33±0.10),[13] all in 10^{-14} $\text{cm}^3\,\text{molecule}^{-1}\,\text{s}^{-1}$. Our room temperature result for Reaction (2) is $(1.79\pm0.35)\times10^{-15}$ and is likewise in agreement with the room temperature value of Miller and Gordon,[14] $(1.64\pm0.07)\times10^{-15}$, both in molecular units. The present LP-ST experiments can be directly compared to the only direct determination at temperatures >500 K, namely that of Adusei and Fontijn.[13] These authors give $k_1=4.4\times10^{-11}\exp(-2568\ \text{K}/T)$ for $291\leqslant T\leqslant1283$ K, and this is only 28%–47% lower than Eq. (8) over our LP-ST range. Since their accuracy is ±26% and ours is ±15%, this magnitude of disagreement is therefore not significant.

The data from all previous direct studies of Reaction (1)[7–13] have been used in an evaluation. Eleven equally spaced in T^{-1} data points were calculated from the analytical expressions from each study over the temperature range of that study, and these were then combined into one database for the entire experimental temperature range 199–2939 K. Since there are no earlier values above 1300 K, the present study was given twice the weight of the earlier studies.[7–13] An attempt was made to fit this database to a three parameter function that is similar to Eq. (8); however, a single equation was not sufficient for the entire range. Therefore, both Arrhenius and three parameter expressions were used depending on the temperature range. The final evaluated rate constant is

$$k_1=2.52\times10^{-11}\times\exp(-2214\ \text{K}/T)\ \text{cm}^3\,\text{molecule}^{-1}\,\text{s}^{-1} \quad (10)$$

for $199\leqslant T\leqslant354$ K and

$$k_1=1.57\times10^{-16}T^{1.72}\times\exp(-1544\ \text{K}/T)\ \text{cm}^3\,\text{molecule}^{-1}\,\text{s}^{-1} \quad (11)$$

for $354\leqslant T\leqslant2939$ K. The evaluation for Reaction (2) only involved the present work and that of Miller and Gordon.[14] The three parameter expression

$$k_2=2.77\times10^{-16}T^{1.62}\times\exp(-2162\ \text{K}/T)\ \text{cm}^3\,\text{molecule}^{-1}\,\text{s}^{-1} \quad (12)$$

over the temperature range 255–3020 K provided an excellent fit. Results for the backreactions H+HCl and D+DCl can easily be derived by dividing Eqs. (10)–(12) by the equilibrium constants, Eqs. (6) and (7).

The data from the individual studies are in good agreement with the Reaction (1) evaluation, Eqs. (11) and (12). The results of Westenberg and de Haas[7] are lower by 4%–13%; those of Watson *et al.*[9] are higher by 2%–38%; those of Lee *et al.*[10] are uniformly lower by 2%; those of Miller and Gordon[11] agree to within ±14%; those of Kita and Stedman[12] are higher by 0%–30%; those of Adusei and Fontijn[13] are uniformly lower by 26%; and those from the present study are lower by 0.2%–11% over the respective temperature ranges. Benson *et al.*[47] derived k_1 values from an indirect method involving a complex chemical mechanism, and they combined their results with earlier indirect[48–50] and direct[7] studies in an evaluation, $7.95\times10^{-11}\exp(-2647\ \text{K}/T)$, for the temperature range, 559–1071 K. This evaluated result from the earlier data is also in quite good agreement with Eq. (11) being higher by only 11%–34%. The Reaction (2) evaluation, Eq. (12), agrees well with both Miller and Gordon[14] (−13 to +2%) and the present Eq. (9) (−9 to +2%), over the respective temperature ranges.

Theory

Tucker *et al.*[5] have reported improved canonical variational theory with least action ground-state transmission coefficient (ICVT-LAG) calculations using 11 different potential energy surfaces (PES). These results were compared to the experimental data obtained before 1985. The greatest success was found by using the Stern–Persky–Klein (SPK) PES.[51] In the present work we have predicted the thermal rate behavior for the title reactions from these 11 surfaces between 200–3000 K. Conventional transition state theory with both Wigner (CTSTW) and Eckart (CTSTE) tunneling corrections is the method of choice in these calculations. With Wigner tunneling, none of these previously described surfaces[5] explain the experimental rate behavior over the entire temperature range. This is illustrated in Figs. 7 to 9 where the evaluated expression for k_1, Eqs. (10) and (11), is compared to the predictions from the CTSTW calculations. Use of the Eckart method improves the results; however, the quality of the fits of theory to experiment is still not good. Examination of these 11 surfaces shows that all give nearly the same value for the protonated transition state moment of inertia, $(1.27\pm0.06)\times10^{-39}$ g cm^2, reflecting relatively little difference in the predicted saddle point configurations. Therefore, the differences in thermal rate constant estimates

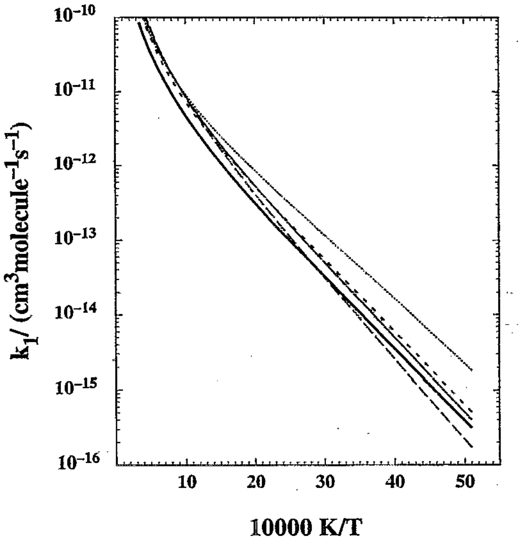

FIG. 7. A comparison between experimental and theoretical rate constants. Four CTSTW theoretical calculations are compared to the experimental evaluation, Eqs. (10) and (11) (the thick solid line), for Cl+H$_2$. The theoretical results are derived from the saddle point properties reported in Table I of Ref. 5. The calculations are identified in the figure with the PES designations given in Ref. 5; i.e., (···) No. 1, (---) SPK, (–––) GSI, and the thin solid line is GSII.

come solely from the electronic energy barrier ($V^{\ddagger}$) and the symmetrical stretching (ν_s), the degenerate bending (ν_b), and the imaginary (ν_i) frequencies, all evaluated at the saddle point. Using Eckart tunneling, we have iteratively varied these four quantities in an attempt to fit both the absolute magnitude and the extent of curvature for both Reactions (1) and (2). The values derived for the deuterated case are of course consistent with the force field appropriate to the protonated case; i.e., the results are in complete accord with the

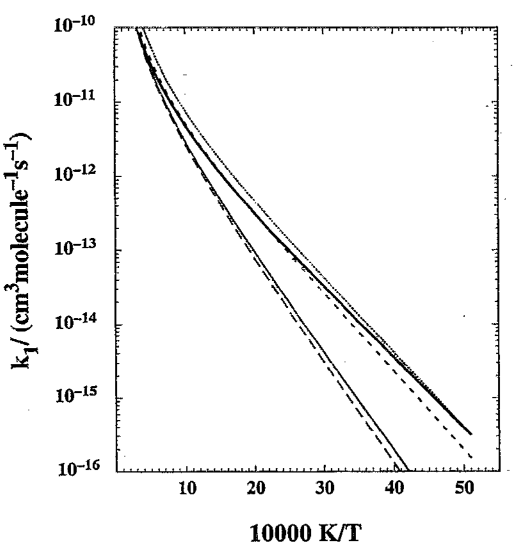

FIG. 8. A comparison between experimental and theoretical rate constants. See the caption to Fig. 7. The CTSTW calculations are (···) No. 2, (---) No. 3, (–––) DIMS, and the thin solid line is DIMA.

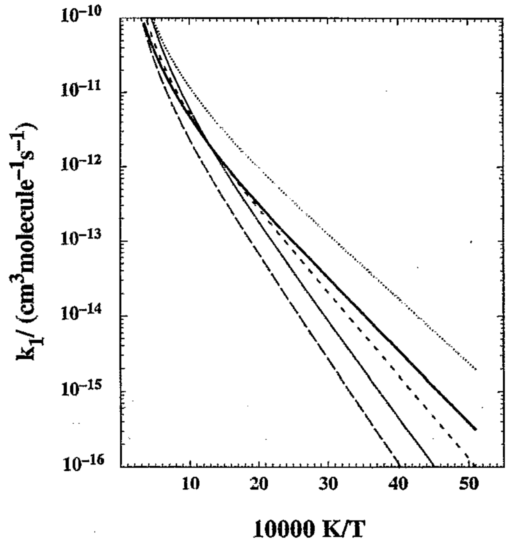

FIG. 9. A comparison between experimental and theoretical rate constants. See the caption to Fig. 7. The CTSTW calculations are (···) AL/AB, (---) DIM3C, and (–––) V. The thin solid line is a CTSTW calculation using the saddle point properties from Ref. 59 (see the text).

Teller–Redlich product rule. The successful model at the CTSTE level of approximation is given in Table V where the overall exoergicity is adjusted to the *JANAF* value.[40] The exact results from these calculations have been fitted to three parameter expressions that are accurate to within ±2%:

$$k_1^{\mathrm{th}}=4.59\times10^{-16}T^{1.588}$$
$$\times\exp(-1682\ \mathrm{K}/T)\ \mathrm{cm}^3\,\mathrm{molecule}^{-1}\,\mathrm{s}^{-1} \quad (13)$$

for $200\leqslant T\leqslant2950$ K and

$$k_2^{\mathrm{th}}=9.20\times10^{-16}T^{1.459}$$
$$\times\exp(-2274\ \mathrm{K}/T)\ \mathrm{cm}^3\,\mathrm{molecule}^{-1}\,\mathrm{s}^{-1} \quad (14)$$

for $255\leqslant T\leqslant3050$ K. Graphical comparisons of the theoretical results to the evaluations, Eqs. (10)–(12), are shown in Figs. 10 and 11, respectively. The Eqs. (10)–(12) experimental and the Eqs. (13) by (14) theoretical kinetic isotope effects, KIE $\equiv (k_{\mathrm{H}_2}/k_{\mathrm{D}_2})$, are compared to one another and to the results of Miller and Gordon[14] and Persky and Klein[52] in Fig. 12.

It is clear from Figs. 10–12 that the present calculations based on the model given in Table V are in complete accord with all of the direct thermal rate constant data within experimental error. The question can then be asked as to whether this is a unique model or not. Since four coupled parameters have been parametrically varied in order to get the fits, we cannot claim complete uniqueness. We do however suggest that the quantities given in Table V cannot be much different from those presented and still give the obviously successful predictions. The data supply severe constraints to the choice of the four parameters in four ways, namely (a) the absolute magnitudes of rate constants and (b) the values relative to one another (i.e., the shape in T^{-1} space) for two sets of data.

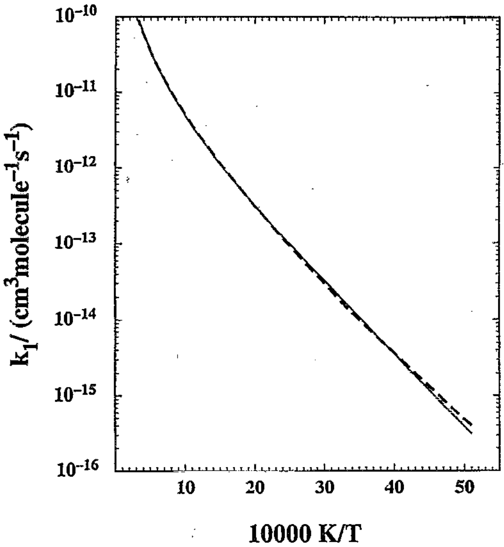

FIG. 10. A comparison between experimental and theoretical rate constants for $Cl+H_2$ over the temperature range $199 \leqslant T \leqslant 2939$ K. The solid line is the evaluation [Eqs. (10) and (11)] based on the results of Westenberg and de Haas (Ref. 7), Watson *et al.* (Ref. 9), Lee *et al.* (Ref. 10), Miller and Gordon (Ref. 11), Kita and Stedman (Ref. 12), Adusei and Fontijn (Ref. 13), and the present study, as described in the text. The dashed line is calculated from the CTSTE model of Table V.

Previous thermal rate constant studies from this laboratory[15–18,28–33] on theoretically important reactions have served as an impetus for continuing theoretical developments using the most modern methods.[15,53–58] Clearly, studies of this type, particularly at high temperatures, supply the best experimental information available for probing moderately high potential barriers in chemical reactions. The present study is another example of how thermal rate data give strong constraints to the theoretical description. In the present work, the description is not rigorous since we have used the approximate CTSTE method. Even though a CTST model for the $D+H_2$[32] and $H+D_2$[33] reactions gave nearly identical results as the CEQB[57] and/or quantum scattering[58] methods (indicating that the reactive flux is close to the minimum energy path), the same might not be true for the present case. Tucker *et al.*[5] have already shown that variational effects can be important here. We note that the Table V model is tighter and has a lower barrier than most of the earlier calculations would indicate. It is not clear whether the present "derivation" of the saddle point properties will be sufficient with a more accurate dynamical theory, and for this reason we suggest that more extensive theoretical investigations using variational transition state, CEQB, and, if possible, quantum scattering calculations be considered. Tunnel-

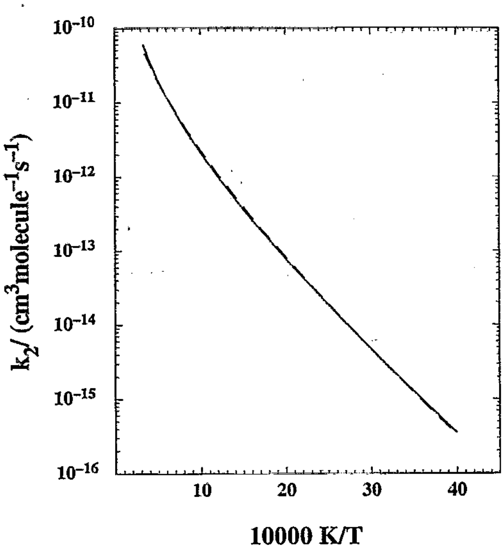

FIG. 11. A comparison between experimental and theoretical rate constants for $Cl+D_2$ over the temperature range $255 \leqslant T \leqslant 3020$ K. The solid line is the evaluation [Eq. (12)] based on the results from the present study and from Miller and Gordon (Ref. 14). The dashed line is the Table V CTSTE model calculation for the deuterated case.

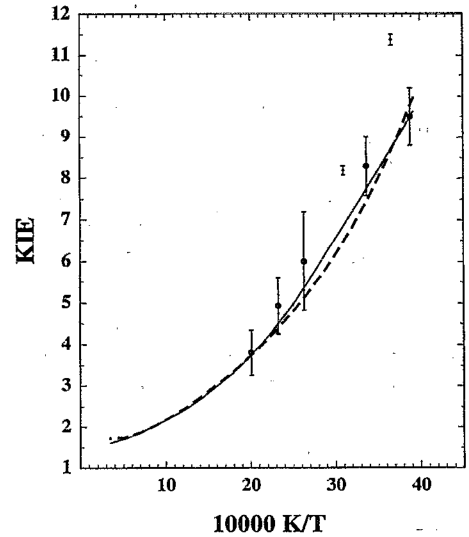

FIG. 12. Experimental (solid line) and theoretical (dashed line) kinetic isotope effect results for the $Cl+H_2$/$Cl+D_2$ system. The data points are from Miller and Gordon (Ref. 14), ●, for $255 \leqslant T \leqslant 498$ K, and Persky and Klein (Ref. 52), •, for 273 and 323 K. The error bars were derived from the corresponding uncertainties in reported rate constants for $Cl+H_2$ and $Cl+D_2$.

TABLE V. Reactant, product, and saddle point properties for the reaction $Cl+H_2$.

Separation (Å)	H_2		HCl	Saddle point
r(H–H)	0.7416			0.9102
r(Cl–H)			1.2745	1.4695
Electronic energy (kcal/mol)	0.0		3.177	6.770
Frequencies (cm^{-1})	H_2	D_2	H···H···Cl	D···D···Cl
ν_s	4395.0	3107.8	2050.0	1475.5
ν_b			782.0(2)	553.8 (2)
ν_i			$1000.0i$	$713.1i$
Zero-point energy (kcal/mol)	6.283	4.443	5.167	2.583

ing corrections with these methods would be far superior to those used here. Of course, such an effort must start with a well determined PES. Harding[59] has performed new CAS singles and doubles with Davidson correction *ab initio* electronic structure calculations, using the cc-pvtz basis set for determining the potential energy surface. The saddle point properties for the protonated case are: $r_{\text{H-H}}=1.002$ Å, $r_{\text{H-Cl}}=1.423$ Å, $\nu_s=1334$ cm^{-1}, $\nu_b=501$ cm^{-1}, $\nu_i=1408i$ cm^{-1}, and $V^{\ddagger}=9.6$ kcal mol^{-1}. This clearly should be the most accurate potential energy calculation on this system to date. However, its use at the CTSTW level of approximation gives poor predictions in comparison to experiment as seen in Fig. 9 (the thin solid line). We believe that the situation might be reconciled if this new PES, perhaps with slight energy scaling, were used in the above-mentioned modern dynamical calculations.[57,58]

ACKNOWLEDGMENTS

The authors wish to thank Dr. L. B. Harding, Dr. A. F. Wagner, Dr. J. P. Hessler, and Professor G. C. Schatz for a thorough reading of the manuscript and helpful suggestions. This work was supported by the U. S. Department of Energy, Office of Basic Energy Sciences, Division of Chemical Sciences, under Contract No. W-31-109-Eng-38.

[1] R. E. Weston, Jr., J. Phys. Chem. **83**, 61 (1979).
[2] W. Nernst, Z. Elektrochem. **24**, 335 (1918).
[3] A. Wheeler, B. Topley, and H. Eyring, J. Chem. Phys. **4**, 178 (1936).
[4] J. Bigeleisen, F. S. Klein, R. E. Weston, Jr., and M. Wolfsberg, J. Chem. Phys. **30**, 1340 (1959).
[5] For a review see, S. C. Tucker, D. G. Truhlar, B. C. Garrett, and A. D. Isaacson, J. Chem. Phys. **82**, 4102 (1985).
[6] F. Westley, D. H. Frizzel, J. T. Herron, R. F. Hampson, and W. G. Mallard, NIST Chemical Kinetics Database—Version 5.0, NIST Standard Reference Database 17, Gaithersburg, MD (1993).
[7] A. A. Westenberg and N. de Haas, J. Chem. Phys. **48**, 4405 (1968).
[8] D. D. Davis, W. Braun, and A. M. Bass, Int. J. Chem. Kinet. **2**, 101 (1970).
[9] R. T. Watson, D. D. Davis, E. S. Machado, B. C. Conaway, and Y. Oh, as reported in Ref. 10.
[10] J. H. Lee, J. V. Michael, W. A. Payne, L. J. Stief, and D. A. Whytock, J. Chem. Soc. Faraday Trans. 1 **73**, 1530 (1977).
[11] J. C. Miller and R. J. Gordon, J. Chem. Phys. **75**, 5305 (1981).
[12] D. Kita and D. H. Stedman, J. Chem. Soc. Faraday Trans. 2 **78**, 1249 (1982).
[13] G. Y. Adusei and A. Fontijn, 25th Symp. (Int.) on Combust. (in press).
[14] J. C. Miller and R. J. Gordon, J. Chem. Phys. **79**, 1252 (1983).
[15] J. V. Michael, J. R. Fisher, J. M. Bowman, and Q. Sun, Science **249**, 269 (1990).
[16] J. V. Michael, Prog. Energy Combust. Sci. **18**, 327 (1992).
[17] See J. V. Michael, in *Advances in Chemical Kinetics and Dynamics*, edited by J. R. Barker (JAI, Greenwich, CT, 1992), Vol. 1, p. 47 for original references.
[18] J. V. Michael and K. P. Lim, Annu. Rev. Phys. Chem. **44**, 429 (1993).
[19] K. P. Lim and J. V. Michael, J. Phys. Chem. **98**, 211 (1994).
[20] J. V. Michael, K. P. Lim, S. S. Kumaran, and J. H. Kiefer, J. Phys. Chem. **97**, 1914 (1993).
[21] J. V. Michael and J. W. Sutherland, Int. J. Chem. Kinet. **18**, 409 (1986).
[22] J. V. Michael, J. Chem. Phys. **90**, 189 (1989).
[23] K. P. Lim and J. V. Michael, 25th Symp. (Int.) on Combust. (in press).
[24] J. V. Michael and R. E. Weston, Jr., J. Chem. Phys. **45**, 3632 (1966).
[25] J. R. Barker and J. V. Michael, J. Opt. Soc. Am. **58**, 1616 (1968).
[26] K. P. Lynch, T. C. Schwab, and J. V. Michael, Int. J. Chem. Kinet. **8**, 651 (1976).
[27] R. G. Maki, J. V. Michael, and J. W. Sutherland, J. Phys. Chem. **89**, 4815 (1985).
[28] J. V. Michael, J. W. Sutherland, and R. B. Klemm, Int. J. Chem. Kinet. **17**, 315 (1985).
[29] J. V. Michael, J. W. Sutherland, and R. B. Klemm, J. Phys. Chem. **90**, 497 (1986).
[30] J. V. Michael and J. W. Sutherland, J. Phys. Chem. **92**, 3853 (1988).
[31] A. N. Pirraglia, J. V. Michael, J. W. Sutherland, and R. B. Klemm, J. Phys. Chem. **93**, 282 (1989).
[32] J. V. Michael and J. R. Fisher, J. Phys. Chem. **94**, 3318 (1990).
[33] J. V. Michael, J. Chem. Phys. **92**, 3394 (1990).
[34] K. S. Shin and J. V. Michael, J. Chem. Phys. **95**, 262 (1991).
[35] K. S. Shin and J. V. Michael, J. Phys. Chem. **95**, 5864 (1991).
[36] K. P. Lim and J. V. Michael, 25th Symp. (Int.) on Combust. (in press).
[37] H. Du and J. P. Hessler, J. Chem. Phys. **96**, 1077 (1992).
[38] D. J. Seery and C. T. Bowman, J. Chem. Phys. **48**, 4314 (1968).
[39] D. L. Baulch, J. Duxbury, S. J. Grant, and D. C. Montague, J. Phys. Chem. Ref. Data **10**, Suppl. 1 (1981).
[40] M. W. Chase, Jr., C. A. Davies, J. R. Downey, Jr., D. J. Frurip, R. A. McDonald, and A. N. Syverud, J. Phys. Chem. Ref. Data **14**, Suppl. 1 (1985).
[41] K. P. Lim and J. V. Michael, J. Chem. Phys. **98**, 3919 (1993).
[42] J. H. Kiefer, R. Sathyanarayana, K. P. Lim, and J. V. Michael, J. Phys. Chem. (in press).
[43] M. A. A. Clyne and W. S. Nip, J. Chem. Soc. Faraday 2 **72**, 838 (1976).
[44] D. A. Whytock, J. H. Lee, J. V. Michael, W. A. Payne, and L. J. Stief, J. Chem. Phys. **66**, 2690 (1977).
[45] K. P. Lim and J. V. Michael, 207th American Chemical Society, Symposium on Combustion Chemistry and Soot Formation, Fuel Chemistry Division (1994), Vol. 39, p. 131.
[46] W. B. DeMore, S. P. Sander, D. M. Golden, R. F. Hampson, M. J. Kurylo, C. J. Howard, A. R. Ravishankara, C. E. Kolb, and M. J. Molina, *Chemical Kinetic and Photochemical Data for use in Stratospheric Modeling*, Evaluation No. 10, JPL Publication 92-20, August 15, 1992.
[47] S. W. Benson, F. R. Cruickshank, and R. Shaw, Int. J. Chem. Kinet. **1**, 29 (1969).
[48] W. H. Rodebush and W. G. Klingelhoefer, J. Am. Chem. Soc. **55**, 130 (1933).
[49] H. Steiner and E. K. Rideal, Proc. R. Soc. London Ser. A **173**, 503 (1939).
[50] P. G. Ashmore and J. Chanmugam, Trans. Faraday Soc. **49**, 254 (1953).
[51] M. J. Stern, A. Persky, and F. S. Klein, J. Chem. Phys. **58**, 5697 (1973).
[52] A. Persky and F. S. Klein, J. Chem. Phys. **44**, 3617 (1966).
[53] T. J. Park and J. C. Light, J. Chem. Phys. **94**, 2946 (1991).
[54] T. J. Park and J. C. Light, J. Chem. Phys. **96**, 8853 (1992).
[55] A. I. Boothroyd, W. J. Keogh, P. B. Martin, and M. R. Peterson, J. Chem. Phys. **95**, 4343 (1991).
[56] D. L. Diedrich and J. B. Anderson, J. Chem. Phys. **100**, 8089 (1994).
[57] D. Wang and J. M. Bowman, J. Phys. Chem. **98**, 7994 (1994).
[58] S. L. Mielke, G. C. Lynch, D. G. Truhlar, and D. W. Schwenke, J. Phys. Chem. **98**, 8000 (1994).
[59] L. B. Harding (private communication).